WEP Warwick Evans Publishing

International Journal of Materials Science and Technology Studies

ISSN: 3006-7693 (Print), ISSN: 3006-3744 (Online)
Volume 5, Number 5, Year 2026
DOI: https://doi.org/10.62051/ijmsts.v5n5.05

Regulation Effect of Amphiphilic Additives on Low-Temperature Performance of Recycled SBS Modified Asphalt under Medium-Low Temperature Conditions

Taoguo Zhu [1,4], Shitong Wu [1], Zhixing Xu [1], Donglin Zhang [1], Xinyue Hou [2], Shida Gong [1], Yufei Ren [3], Fenfen Meng [1], Kai Zhang [1], Yue Zhang [1], Xiaoya Shen [1,*]

[1] School of Civil Engineering, Lanzhou Bowen University of Science and Technology, Lanzhou 730100, China

[2] Gansu University of Political Science and Law, Lanzhou, China

[3] Guangzhou Maritime University, Guangzhou, China

[4] Shaanxi Highway Society, Xi'an, China

*Corresponding Author: Xiaoya Shen

ABSTRACT

Conventional high-temperature thermal regeneration typically induces secondary chain scission of residual SBS; reducing the regeneration temperature alone elevates asphalt viscosity, suppresses interfacial diffusion, and precludes interfacial wetting-dispersion-swelling of residual SBS. Achieving homogeneous dispersion of residual SBS and satisfactory low-temperature crack resistance under reduced temperatures remains a technical challenge in road regeneration materials, particularly in cold regions. In this study, an amphiphilic composite regenerant from light oil fractions and nonionic surfactants was used to regenerate RTFO+PAV-aged SBS-modified asphalt at 120–140 °C. DSR, BBR, ATR-FTIR, and SEM were utilized to investigate the effects of regeneration temperature and additive dosage on physical properties, low-temperature creep behavior, functional group evolution, and micromorphology. At 130 °C and 6 wt% dosage, the 60-second creep modulus decreased by 17.2% relative to the 170 °C group, while the m-value at 60 s increased by 15.2%. FTIR analysis shows no increment in the carbonyl index, and the butadiene index remained higher than that of the high-temperature group. SEM reveals that the SBS dispersed phase tended toward continuous distribution, with reduced interface delineation. Samples with 8 wt% SBS showed enhanced recovery of physical properties at 140 °C; however, their low-temperature creep resistance and long-term aging performance require further validation. These findings indicate that amphiphilic additives enhance interfacial wetting and dispersion between asphalt and residual SBS, improving low-temperature deformation resistance under reduced processing temperatures. This study proposes a physically compatible blending approach for low-carbon recycling of aged SBS-modified asphalt.

KEYWORDS

SBS-modified asphalt; Medium- and low-temperature recycling; Amphiphilic additives; Interfacial wetting; Low-temperature crack resistance; Microstructural characterization

1. INTRODUCTION

Due to its excellent viscoelasticity and deformation recovery capability, SBS-modified asphalt is widely used in high-grade pavements. [3, 17] During long-term service, thermal-oxidative aging causes the SBS molecular chains to break down and reduces the compatibility between the asphalt phase and the polymer phase, [11, 13] leading to a decline in pavement performance—particularly

Content from this work may be used under the terms of CC BY-NC 4.0 licence (https://creativecommons.org/licenses/by-nc/4.0/). Published by Warwick Evans Publishing.

low-temperature crack resistance. [4] Asphalt recycling is an important approach for the resource-based utilization of waste modified asphalt. Conventional recycling processes typically involve mixing a recycling agent with aged asphalt at 160–180 °C. [11] Although this process can partially restore the basic physical properties of the asphalt by replenishing light components, the relatively high processing temperature induces secondary thermal-oxidative degradation of the residual SBS chains, further compromising the enhanced interfacial compatibility of residual SBS.To reduce the processing temperature, researchers have proposed approaches based on warm-mix recycling and low-temperature recycling. However, existing studies on low-temperature recycling have primarily focused on adjusting construction temperatures and evaluating macroscopic pavement performance; systematic discussion remains lacking regarding how the increase in asphalt viscosity at low temperatures affects the migration and dispersion of fractured SBS chains, as well as the relationship between interfacial state and low-temperature creep behavior. Amphiphilic molecules contain both lipophilic and hydrophilic groups, which can reduce the interfacial tension of multiphase systems and improve wettability. [18] In this study, light oil fractions were blended with nonionic surfactants to form an amphiphilic rejuvenating agent, which was used to rejuvenate SBS-modified asphalt aged through RTFO at temperatures ranging from 120 °C to 140 °C. [20] Using multiple-scale characterization techniques—including DSR, BBR, ATR-FTIR, and SEM—the influence of rejuvenation temperature and additive dosage on rejuvenation performance was investigated, with a focus on answering the following questions: ① Under the action of an amphiphilic additive, can low-temperature creep performance comparable to, or even superior to, that achieved through high-temperature rejuvenation be attained under medium- and low-temperature conditions? ② How do processing temperature and additive dosage affect the interfacial state of the asphalt–residual SBS system? ③ What are the applicable boundaries for this physical rejuvenation pathway?

2. EXPERIMENT DESIGN

2.1. Raw Materials

The base asphalt is Sinopec Grade 70A road petroleum asphalt; SBS is a linear styrene–butadiene–styrene block copolymer (YH-792, Baling Petrochemical), with a dosage of 4.0% by mass of asphalt, and unaged SBS-modified asphalt is prepared using a high-speed shear process (175 °C, 5,000 rpm, 45 min). [5] The regenerative agent oil is furfural-extracted aromatic oil (Maoming Petrochemical); the surfactant is octylphenol polyoxyethylene ether OP-10 (Sinopharm Group, chemical grade) [2]. An amphiphilic regenerative agent is prepared by mixing the aromatic oil OP-10 with the surfactant at a mass ratio of OP-10:9:1 and stirring at 60 °C for 30 min. The technical specifications for the primary raw materials are provided below Table 1.

Table 1. Main raw material technical specifications

material	indicator	test value	Specification scope
Grade A matrix asphalt No. 70	Penetration depth (25°°C)	68.5	60~80
	softening point/°C	48.2	≥46
	Ductility (10 °C)/cm	26.4	≥20
	Wax content /%	1.8	≤2.2
	Flash point/°C	268	≥260
	Density (15 °C)	1.032	—
SBS-modified asphalt (unaged, 4% linear	Penetration depth (25 °C)	58.6	—
	softening point/°C	68.5	≥55
	Ductility (5 °C)/cm	42.3	≥30
	Dynamic viscosity (135 °C)	1.85	≤3.0
	Elastic Recovery (25 °C)/%	78	≥70
	Segregation (48 h softening point difference)/°C	1.3	≤2.5
Aromatic oil (furfural-extracted oil)	Density (15 °C)	0.985	—
	Dynamic viscosity (100 °C)	38.6	20~60
	Flash point/°C	226	≥220
	Aniline point/°C	32.5	—
	Saturates/%	18.2	—
	Aromatic content/%	58.6	—
	Gum/%	21.8	—
	asphaltene/%	1.4	≤3
OP-10 (octylphenol polyoxyethylene ether)	appearance	pale yellow viscous liquid	—
	HLB value	13.3	—
	Cloud Point (1% aqueous solution)	65	—
	pH (1% aqueous solution)	6.2	5~7
	active matter content/%	≥99	—
	flash point/°C	218	—
Amphiphilic regenerator (aromatic oil: OP-10 = 9:1)	Density (25 °C)	0.978	—
	Dynamic viscosity (60 °C)	286	—
	Flash point /°C	232	—
	Saturates/%	17.6	—
	Aromatics/%	57.2	—
	Colloid/%	23.5	—
	asphaltene/%	1.7	—

2.2. Sample Preparation Protocol

The original SBS-modified asphalt was aged by RTFO followed by PAV to obtain the aged masterbatch (R1). Regeneration parameters were: processing temperatures of 120, 130, and 140 °C; regenerant dosages of 4, 6, and 8 wt%; mixing at 1500 r/min for 30 min. Three control groups were established: CK1 (aged asphalt heated only at 130 °C, 30 min — sole-heating control); CK2 (aged asphalt blended with neat aromatic oil at 130 °C — surfactant-free control); R2 (170 °C [1], 6 wt% — conventional high-temperature regeneration control). Specimens are designated R0 (unaged virgin SBS-modified asphalt), R1 (aged masterbatch), R3–R11 (gradient regeneration groups: 3 temperatures × 3 dosages, Table 2), and R2, CK1, CK2 (controls). R2 is an independent high-temperature control and is NOT part of the R3–R11 gradient series. A total of 12 specimen groups were investigated.

Table 2. Gradient regeneration matrix (R3–R11)

Dosage	120°C	130°C	140°C
4wt%	R3	R6	R9
6wt%	R4	R7	R10
8wt%	R5	R8	R11

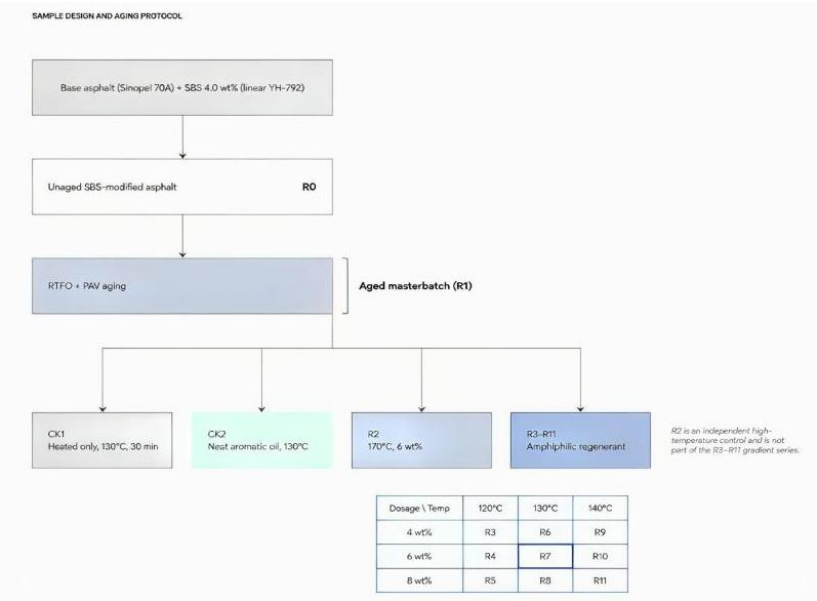


Figure 1. Design and aging protocol of the recycled SBS-modified asphalt

2.3. Test Method

Macroscopic conventional property characterization: Penetration, softening point, ductility, and Brookfield rotational viscosity were determined in strict compliance with the JTG E20-2011 standard. No fewer than three replicate specimens were tested per group, with results expressed as mean values accompanied by corresponding standard deviations. Rheological property analysis: Dynamic Shear Rheometer (DSR) temperature sweep tests were conducted to measure the complex shear modulus and phase angle. Bending Beam Rheometer (BBR) tests were performed to derive the creep stiffness (S) and creep rate (m) at temperatures of −12 °C, −18 °C, and −24 °C. Supplementary rheological assessments were carried out on specimens after long-term aging induced by Pressure Aging Vessel (PAV), so as to evaluate the durability performance. Microstructural characterization: Fourier Transform Infrared (FTIR) spectroscopy was performed over a scanning range of 4000–400 cm^{-1}, with a reference spectrum of the pure rejuvenator collected simultaneously for subsequent background signal elimination via differential spectral subtraction. Scanning Electron Microscopy (SEM) was employed to examine the micro-morphology of sample fracture surfaces, and the particle size distribution of the dispersed phase was statistically analyzed.

3. RESULTS AND DISCUSSION

3.1. Conventional Macroscopic Properties

Table 3. Conventional Physical Properties of Recycled Asphalt

Number	Condition	Penetration depth / (0.1 mm)	Softening point / ℃	Ductility (15 ℃) / cm	Viscosity (135 ℃) / (Pa·s)
R0	Unaged, as-is	70.1±1.4	47.2±0.3	>100	0.42±0.02
R1	aging blank	33.5±1.2	58.2±0.5	9.6±1.8	1.15±0.04
R2	170 ℃, 6%	61.8±1.3	51.9±0.4	43.8±2.0	0.82±0.03
R3	120 ℃, 4%	48.6±1.1	54.3±0.5	24.8±1.9	0.89±0.03
R4	120 ℃, 6%	62.3±1.4	51.8±0.4	46.2±2.1	0.71±0.03
R5	120 ℃, 8%	70.2±1.5	49.2±0.4	68.4±2.4	0.58±0.02
R6	130 ℃, 4%	50.2±1.2	53.9±0.4	26.3±2.0	0.86±0.03
R7	130 ℃, 6%	64.1±1.3	51.4±0.4	48.5±2.2	0.68±0.03
R8	130 ℃, 8%	72.0±1.5	48.9±0.4	71.2±2.5	0.56±0.02
R9	140 ℃, 4%	51.4±1.2	53.6±0.4	27.6±2.0	0.84±0.03
R10	140 ℃, 6%	65.8±1.4	51.0±0.4	51.3±2.3	0.66±0.03
R11	140 ℃, 8%	73.6±1.5	48.6±0.4	74.0±2.6	0.54±0.02
CK1	130 ℃, No regenerant	32.1±1.2	57.5±0.5	10.8±1.7	1.12±0.04
CK2	130 ℃, Neat aromatic oil	47.3±1.2	52.8±0.4	25.1±1.9	0.84±0.03

As evident from: the sole heat-treated group CK1 exhibits negligible performance recovery, indicating that thermal action alone is insufficient to substantially restore the colloidal structure of aged asphalt. The pure aromatic oil group CK2 demonstrates partial performance improvement, yet its ductility enhancement remains limited. For asphalt samples incorporated with the amphiphilic rejuvenator, increasing rejuvenator dosage and moderately elevating treatment temperature result in raised penetration and ductility, alongside reduced softening point and viscosity. R11 (140 ℃, 8%) achieves the minimum viscosity and maximum ductility, verifying that high rejuvenator dosage and relatively elevated temperature facilitate asphalt softening. However, excessive rejuvenator dosage introduces an excess of light fractions, which undermines the high-temperature deformation resistance of the asphalt system. Comprehensively considering the balance between high-temperature viscosity and low-temperature deformation capacity, R7 (130 ℃, 6%) delivers the optimal overall performance.

3.2. Low-temperature Creep Performance (BBR)

Table 4. BBR results for each group of samples (60 s, n=3)

Number	−12 ℃ S/MPa	−12 ℃ m	−18 ℃ S/MPa	−18 ℃ m
R0	82±6	0.49±0.02	165±12	0.40±0.02
R1	175±11	0.33±0.02	312±18	0.27±0.02
R2	118±9	0.41±0.02	215±14	0.33±0.02
R7	92±7	0.45±0.02	178±11	0.38±0.02
R8	88±6	0.41±0.02	166±10	0.36±0.02
R10	105±8	0.42±0.02	185±12	0.36±0.02
R11	82±6	0.38±0.02	155±10	0.35±0.02
CK1	168±10	0.34±0.02	298±17	0.28±0.02
CK2	125±9	0.40±0.02	232±14	0.33±0.02

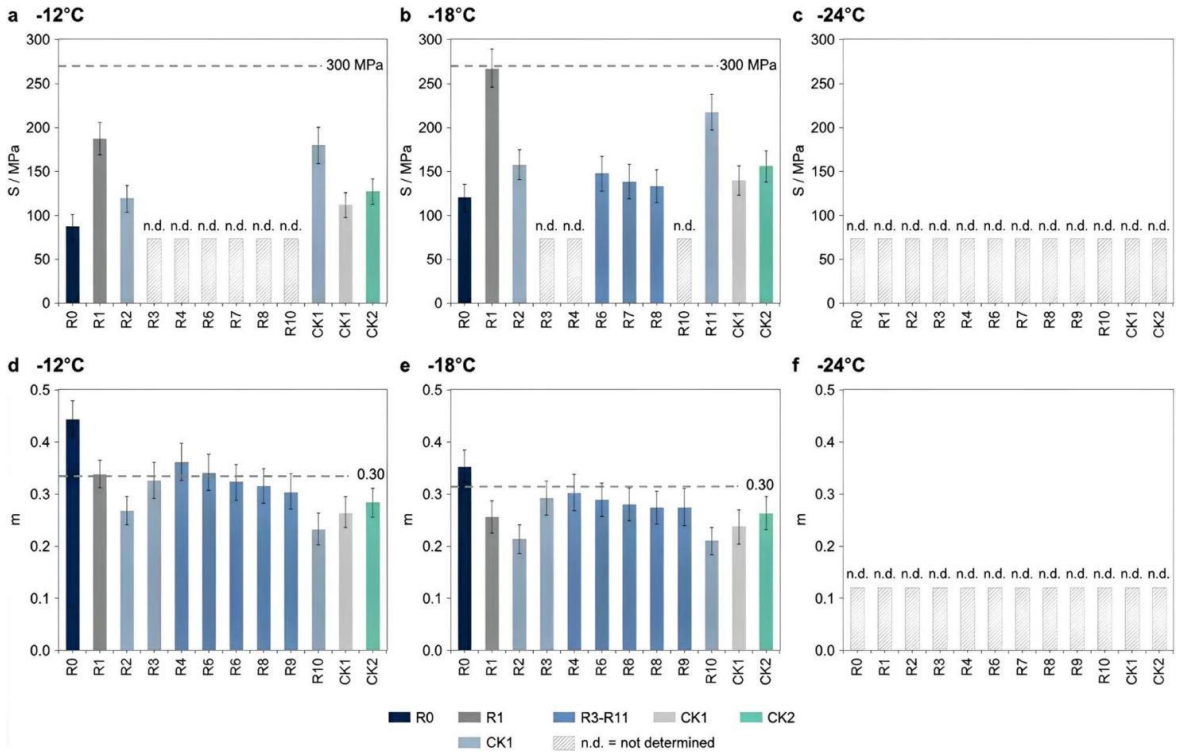


Figure 1. Low-temperature creep properties of all specimen groups by BBR.

At −18 °C, the creep stiffness S of the aged specimen R1 was 312 MPa and the creep rate m was 0.27, failing to meet the general evaluation criterion for asphalt low-temperature performance, which requires $S \leq 300$ MPa and $m \geq 0.30$. After processing at 170 °C with a 6% additive content, the creep stiffness S of specimen R2 decreased to 215 MPa, while the creep rate m increased to 0.33; for specimen R7, the creep stiffness S was further reduced to 178 MPa and the creep rate m increased to 0.38, representing reductions of 17.2% and increases of 15.2%, respectively, compared with specimen R2; these differences were statistically significant ($p < 0.05$). It should be noted that although specimen R11 exhibited the lowest creep stiffness S (155 MPa), its creep rate m was only 0.35, lower than that of specimen R7 (0.38); this indicates that a high oil content can reduce asphalt hardness and stiffness, but does not simultaneously enhance its stress relaxation capacity. The test results for specimen CK1 were similar to those of R1, confirming that simple heating provides limited improvement to asphalt low-temperature performance; the creep stiffness S and creep rate m of specimen CK2 fell between those of R1 and R7, indicating that oil swelling contributes to asphalt low-temperature performance, while the interfacial regulatory effect of surfactants can further increase the creep rate m.

3.3. High-temperature Rheological Properties (DSR)

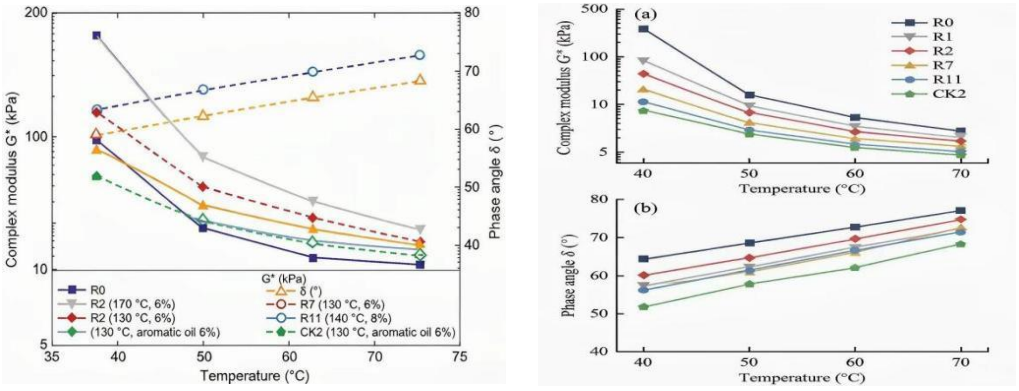


Figure 2. a. Combined Dual Y-Axis Plot b. top and bottom panel diagram

Results from the DSR temperature scanning test indicate that aging treatment increases the complex shear modulus G of the asphalt, reduces the phase angle δ, and increases the proportion of the elastic component. After the addition of an amphiphilic rejuvenating agent, the complex shear modulus G of the asphalt decreases while the phase angle δ recovers; under the same addition level, the complex modulus of the 130 °C rejuvenated sample retains a slightly higher degree within the medium-temperature range than that of the 170°C rejuvenated sample. This result is consistent with the inference that a lower processing temperature can slow the secondary oxidation of SBS.

3.4. Infrared Spectroscopy (FTIR)

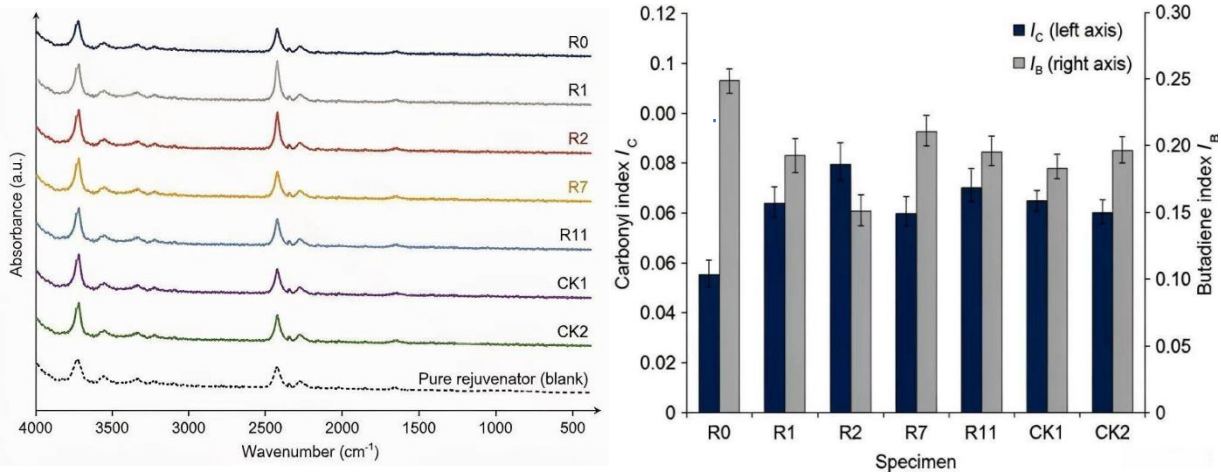


Figure 3. a. ATR-FTIR spectrum comparison chart b. Bar chart of the carbonyl index and butadiene index

Table 5. Index and butadiene index of samples from each group

Number	IC	IB
R0	0.052±0.003	0.238±0.008
R1	0.081±0.004	0.192±0.006
R2	0.094±0.005	0.167±0.006
R7	0.079±0.004	0.211±0.007
R11	0.087±0.005	0.196±0.006
CK1	0.083±0.004	0.188±0.006

FTIR shows that for the 130 °C regenerated specimen (R7), the carbonyl index (IC = 0.079) shows no further increase relative to the aged masterbatch R1 (IC = 0.081), whereas the 170 °C control R2 exhibits a higher IC (0.094), indicating secondary oxidation of SBS at elevated temperature. The butadiene index of R7 (IB = 0.211) remains markedly higher than that of R2 (IB = 0.167), confirming suppressed oxidative chain scission of residual SBS at 130 °C, validating that the high-temperature regeneration process is concomitant with secondary oxidation reactions of SBS components. For the 130 °C regeneration group, IC was 0.079 with no observable further increment, and I_B reached 0.211, which was markedly higher than that of the 170 °C high-temperature treatment group. It should be emphasized that the amphiphilic regeneration system employed in this study contains no reactive functional groups. No new C–O–C ether bond formation peaks or characteristic peaks indicative of epoxy ring opening were identified via Fourier transform infrared spectroscopy (FTIR). Accordingly, the elevation of I_B is primarily ascribed to the suppression of further oxidative chain scission of residual SBS by the lower processing temperature, alongside the substantial enhancement in detection sensitivity for characteristic peaks after the uniform dispersion of agglomerated SBS particles, rather than the occurrence of covalent reconnection reactions within SBS molecular chains.

3.5. Microscopic Morphology (SEM)

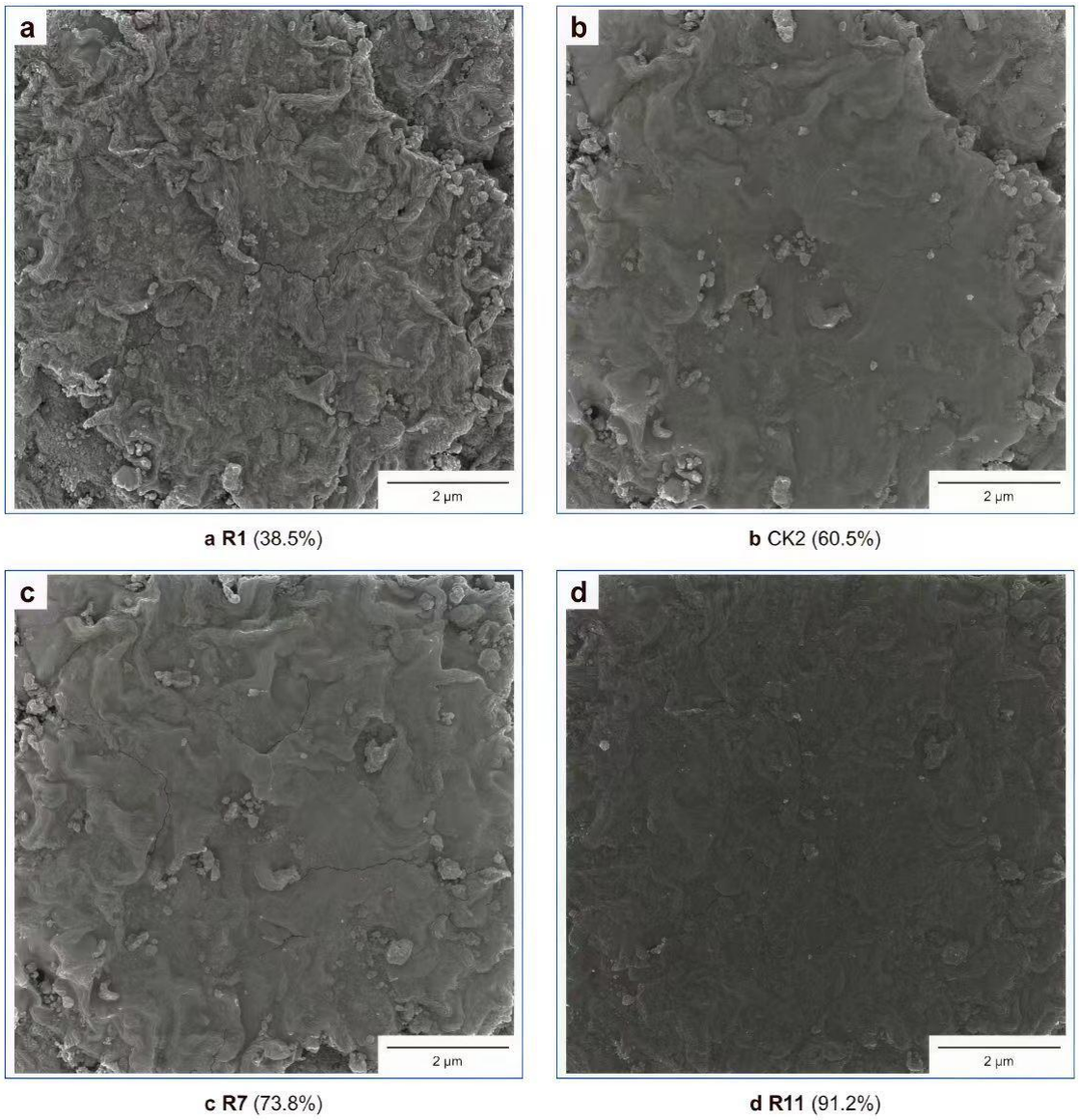


Figure 4. Comparative SEM morphology images of cross-sections R1, CK2, R7, and R11

Table 5. SEM Quantitative Statistics and Surface Tension

Number	Surface tension/(mN·m^{-1})	phase area/%	average grain diameter/μm	grain size CV/%	Interface repair degree/%
R0	38.5	12.8	15.2	18.5	100
R1	41.2	5.6	8.4	42.3	38.5
R2	36.8	8.9	12.6	33.6	64.2
R7	27.3	10.2	12.6	26.1	73.8
R11	26.5	12.4	14.8	19.3	91.2
CK2	33.5	8.2	11.5	30.2	60.5

The surface tension of aged asphalt increased to 41.2 mN/m; after the introduction of an amphiphilic additive, the surface tension of the R7 specimen decreased to 27.3 mN/m, while that of the R11 specimen was 26.5 mN/m, indicating that nonionic surfactants can effectively reduce the surface free energy of asphalt. [18, 19] Scanning electron microscopy (SEM) observations revealed that in the

aged specimens, the SBS phase appeared as irregular fragments with a broad particle-size distribution; in the CK2 specimen, only slight swelling of aggregated particles was observed; in the R7 specimen, the particle size of the dispersed phase became more uniform, and the interface edges became less distinct; the R11 specimen exhibited the best dispersion performance, although a small number of locally oil-rich regions were observed in cross-sections.

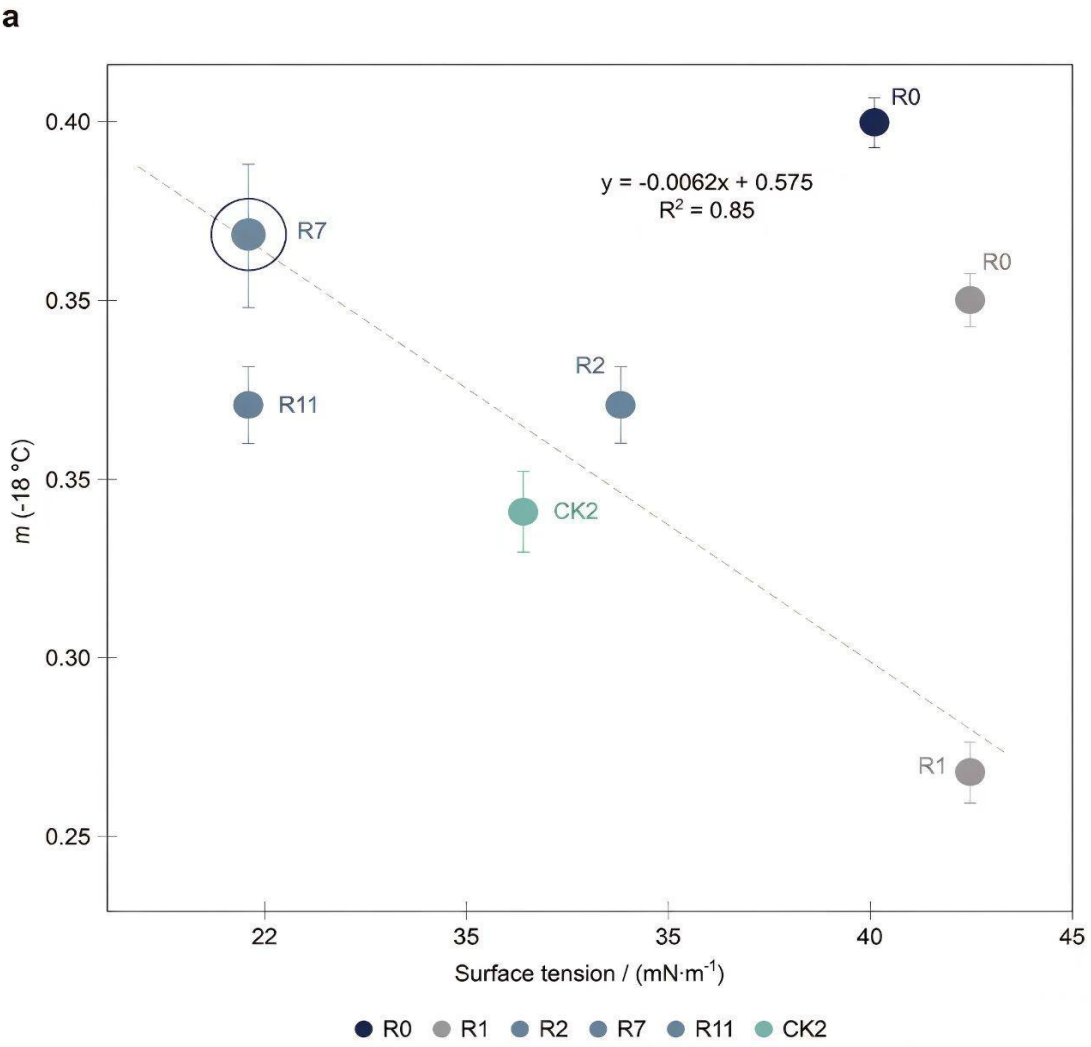


Figure 5. Surface tension vs. m-value regression scatter plot

3.6. Performance After Additional PAV re-aging

Table 6. Performance of BBR (−18 °C) and the mixture after long-term aging of PAV

Indicator	R0	R1	R2	R7	R11
PAV post S/MPa	245±15	385±22	310±18	235±14	264±16
PAVbehindm	0.32±0.02	0.22±0.02	0.26±0.02	0.33±0.02	0.31±0.02
Low-temperature bending failure strain/με	3250±180	1 780±120	2 350±150	2 820±160	2 650±150
Tire rut dynamic stability / (cycle·mm^{-1})	3150±200	4 620±280	2 980±180	2 750±170	2 480±160
Freeze–thaw splitting strength ratio/%	88.5±2.1	76.2±2.5	80.3±2.2	85.6±2.0	82.4±2.1

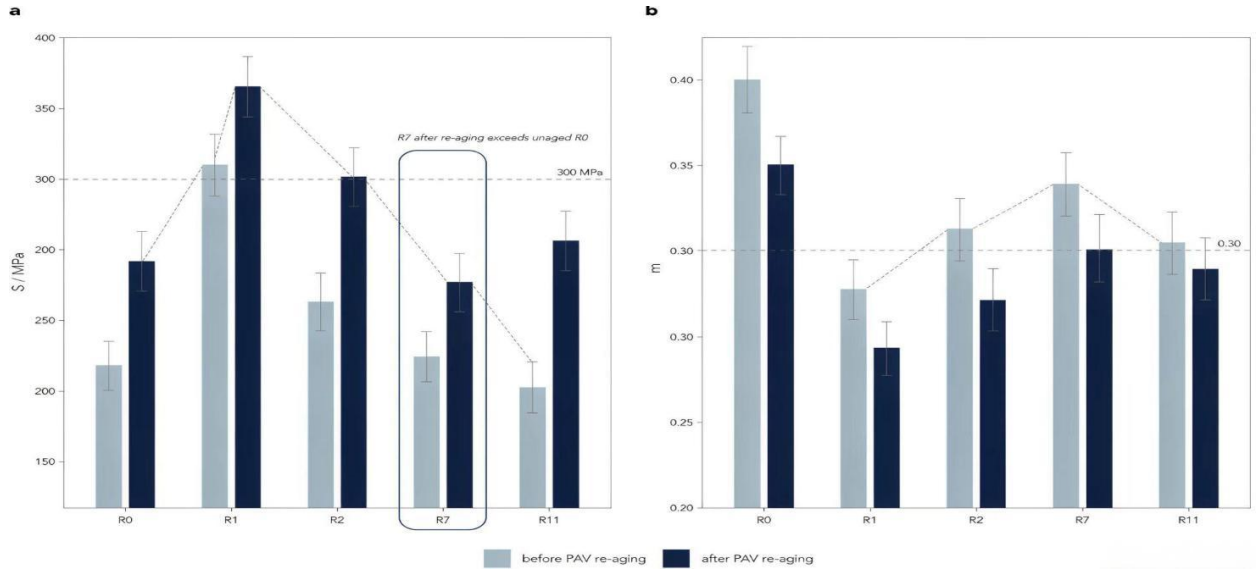


Figure 6. PAV front-to-rear paired comparison image

After an additional PAV cycle treatment, the creep modulus (S) of the R2 specimen increased to 310 MPa, while the creep rate (m) decreased to 0.26; for the R7 specimen, S was 235 MPa and m was 0.33, indicating superior long-term performance retention compared with the high-temperature rejuvenated group; the R11 specimen exhibited excellent initial performance, but after PAV treatment, its S increased to 264 MPa, resulting in a greater degree of performance degradation than that of R7; this phenomenon is associated with the greater susceptibility of excess light-weight components to oxidative volatilization. At the asphalt mixture level, the low-temperature flexural failure strain of R7 was 2820 με, and its freeze–thaw splitting strength ratio was 85.6% [8], meeting road performance requirements; its rutting dynamic stability was slightly lower than that of R2, but remained within an applicable range.

3.7. Regenerative Mechanism

The regeneration effect of the amphiphilic regenerator can be decomposed into three coupled mechanisms: ① Aromatic oil components can replenish the light-weight fractions [11, 12] lost during asphalt aging, thereby reducing the viscosity of the asphaltene phase [14]; ② OP-10, acting as a nonionic surfactant [18], accumulates at the interface between the asphalt phase and the fragmented SBS phase [19], reducing the interfacial surface tension from 38.5 mN/m to 27.3 mN/m, which promotes the delamination of aggregated SBS particles and achieves uniform dispersion; ③ A processing temperature of 130 °C can significantly reduce the degree of thermal-oxidative degradation of residual SBS compared with 170 °C [15]. The synergistic action of these three mechanisms results in R7 specimens exhibiting superior m-values—used to characterize stress relaxation capacity—compared with the high-dosage, high-processing-temperature R11 group. The entire regeneration process is primarily driven by physical swelling and interfacial dispersion; spectral analysis in this study found no direct evidence of the formation of new covalent bonds [6]. Consequently, this physical rejuvenation mechanism should not be described as "polymer physical swelling-dispersion of residual SBS" or physical swelling of fragmented SBS domains [16].

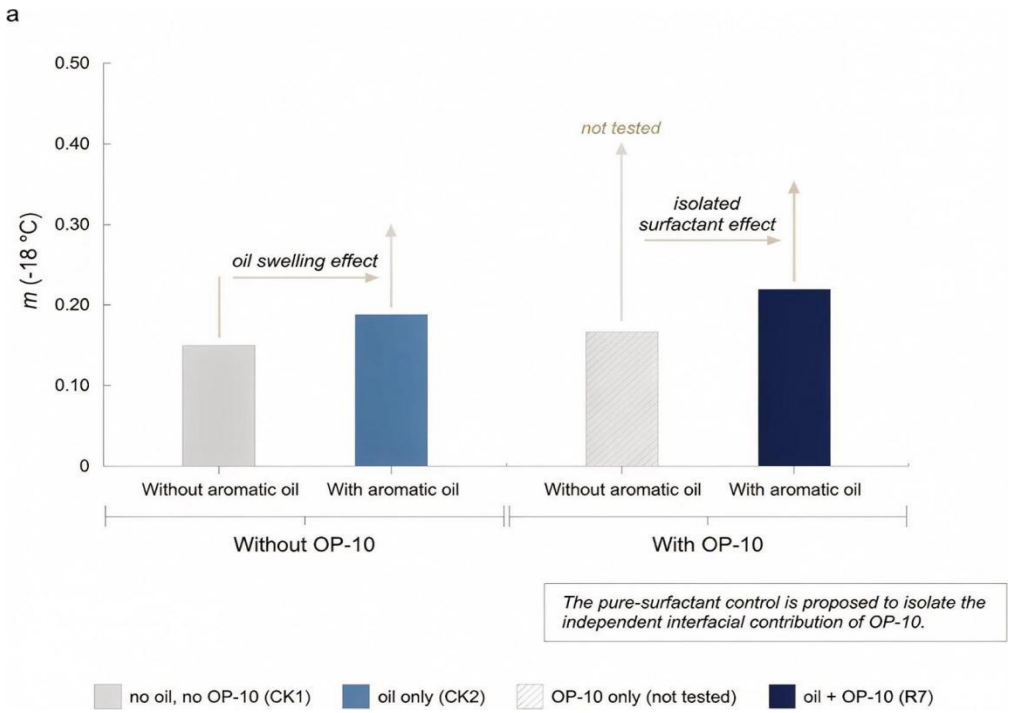


Figure 7. 2×2 Factor Comparison Diagram

4. ANALYSIS AND DISCUSSION

4.1. Physical Mechanism of Action of Amphiphilic Agents

Distinct from the epoxidized soybean oil/triphenylphosphine catalytic restoration pathway proposed by Wei et al. (2020) [16] and the epoxy group-based chemical reconnection strategy reported by Chiang et al. (2025) [13], the aromatic oil/OP-10 system employed in this investigation contains no reactive functional groups, with its physical rejuvenation mechanism operating through three coupled effects: (i) the aromatic oil replenishes the light fractions volatilized during aging, thereby reducing the viscosity of the asphalt matrix; (ii) OP-10 enriches at the asphalt-residual SBS interface, reducing interfacial surface tension from 38.5 mN/m to 27.3 mN/m and enhancing the wetting and dispersion of SBS particles; (iii) the 130 °C processing temperature mitigates thermo-oxidative degradation of residual SBS relative to the 170 °C condition, as evidenced by a decrease in the carbonyl index IC from 0.094 to 0.079. The synergistic interaction of these three effects results in specimen R7 exhibiting superior stress relaxation performance (quantified by the m value) compared to the high-dose, high-temperature group (R11) [7, 9], despite the latter displaying a lower S value.

4.2. Differences From Existing Research

Existing warm-mix recycling studies primarily target reducing construction temperatures, while reactive rejuvenators rely on chemical reconnection [10]. The marginal contribution of this study lies in: utilizing nonionic surfactants as a physical interface regulation method, without introducing reactive groups, achieving low-temperature creep and long-term aging performance at 130 °C that surpasses that of treatments using the same additives at 170 °C.

5. CONCLUSION

Simple thermal activation treatment (CK1) exhibits clear limitations in restoring the performance of aged asphalt; while a single aromatic oil component (CK2) can replenish the light-weight components lost during aging and restore the penetration index, its dispersing effect on fragmented SBS phases is

insufficient; in contrast, amphiphilic rejuvenators can significantly enhance the compatibility between the asphalt phase and residual SBS phases through interfacial wetting and dispersion effects. (2) Within the parameter range tested in this study, a processing temperature of 130 °C and a dosage of 6 wt% (corresponding to the R7 group) achieved the most favourable balance among the tested groups between low-temperature performance, high-temperature performance, and long-term anti-aging capability: at -18 °C, the creep stiffness S decreased by 17.2% and the m-value increased by 15.2% relative to the 170 °C/6 wt% control (R2) ($p < 0.05$). Although the R11 group (140 °C, 8 wt%) exhibited lower initial low-temperature stiffness, its stress relaxation capacity was weaker, resulting in more pronounced performance degradation after additional PAV re-aging. However, low-temperature data were not available for all gradient groups (R3–R6 and R9), and the generality of this conclusion should therefore be further verified over a wider parameter range. (3) After subtracting the baseline signal of the rejuvenator, Fourier transform infrared spectroscopy (FTIR) detected no characteristic signals indicative of the formation of new covalent bonds; the increase in the carbonyl index (I_C) primarily stems from the inhibitory effect of the lower processing temperature on the oxidative degradation of residual SBS and the dispersing effect on agglomerated particles, rather than from the reconnection of chemical covalent bonds. (4) This study currently represents an experimental investigation at the binder scale; while the road performance of the asphalt mixtures has been preliminarily validated, Further performance testing under different temperature gradients in cold regions and long-term field monitoring are still required to further define the engineering applicability boundaries of this rejuvenation technology.

ACKNOWLEDGEMENTS

The authors gratefully acknowledge the support of the experimental platform and testing facilities provided by Lanzhou Bowen College of Science and Technology. We thank Lanzhou Bowen College of Science and Technology for assistance with the conventional property tests, dynamic shear rheometer (DSR), bending beam rheometer (BBR), attenuated total reflectance Fourier transform infrared (ATR-FTIR) spectroscopy, and scanning electron microscopy (SEM) characterizations.

REFERENCES

[1] Li, T. H. (2025). Preparation and performance study of acetylated lignin/pine needle oil-modified asphalt. Nanjing Forestry University. https://doi.org/10.27242/d.cnki.gnjlu.2025.001042

[2] Liu, Y. T., & Li, W. (2025). Study on the properties of calcium sulfate whiskers/bio-oil modified asphalt. Fujian Building Materials, (11), 1–4. (in Chinese)

[3] Li, L. (2025). Research on resin-modified asphalt and its application in drainage-type ultra-thin asphalt coverings. Nanjing Forestry University. https://doi.org/10.27242/d.cnki.gnjlu.2025.000800

[4] Liu, D. K., Wang, W., Deng, J. L., & Chen, L. (2025). Modified matrix asphalt based on polyethylene and rubber powder and its performance tests. Polyester Industry, 38(3), 27–29. https://doi.org/10.3969/j.issn.1008-8261.2025.03.009. (in Chinese)

[5] Chen, G. Q. (2025). Synthesis of dicarboxylic acid-type bio-based polyamide and research on its application as a hot-melt adhesive. Guilin University of Technology. (in Chinese)

[6] Luo, X. (2025). Study on the recycling mechanism of rubber asphalt mixtures based on the molecular diffusion fusion theory. Chongqing Jiaotong University. (in Chinese)

[7] Shan, D. (2021). Study on the properties and mechanisms of recycled bitumen using rubber powder. Beijing University of Chemical Technology. https://doi.org/10.26939/d.cnki.gbhgu.2021.000626. (in Chinese)

[8] Sha, Y. H., & Song, W. J. (2024). Study on the properties of modified asphalt using waste soybean oil from food processing wastewater. Contemporary Chemical Engineering, 53(1), 68–72. (in Chinese)

[9] Yin, P., & Pan, B. F. (2023). Establishment and evaluation of a high-temperature constitutive model for recycled asphalt based on MSCR. Journal of Building Materials, 26(5), 499–507. https://doi.org/10.3969/j.issn.1007-9629.2023.05.007. (in Chinese)

[10] Lin, M. L. (2019). Study on the rheological properties and low-temperature performance of DIBCH plasticizer-modified asphalt. Chang'an University. (in Chinese)

[11] Hong, W., Mo, L., Pan, C., Riara, M. M., Wei, M., & Zhang, J. (2020). Investigation of rejuvenation and modification of aged asphalt binders by using aromatic oil-SBS polymer blend. Construction and Building Materials, 231, 117154. https://doi.org/10.1016/j.conbuildmat.2019.117154

[12] Xia, X., Tang, D., Wang, P., & Zhao, Y. (2025). Comparative analysis of aged-SBSMA regeneration in hot in-place recycling: Individual and coupled effects of aromatic oil and SBS/SBR polymer modifiers. Journal of Materials in Civil Engineering. https://doi.org/10.1061/jmcee7.mteng-19491

[13] Xie, Z., Shan, L., Yang, H., Liu, S., Sun, C., & Cui, H. (2025). Development of an environmentally friendly composite rejuvenator for SBS-modified asphalt binder. Construction and Building Materials, 471, 140445. https://doi.org/10.1016/j.conbuildmat.2025.140445

[14] Huo, J., Zhang, X., Liu, F., & Li, Y. (2024). Rejuvenation performance and mechanism of aged SBS modified asphalt rejuvenated by bio-oil based rejuvenators. Construction and Building Materials, 457, 139366. https://doi.org/10.1016/j.conbuildmat.2024.139366

[15] Sun, C., Li, Q., Liang, C., & Wang, H. (n.d.). Improving compatibility of devulcanized rubber/bio-oil composite rejuvenated SBS modified asphalt using maleic anhydride-grafted polymer. Construction and Building Materials.

[16] Wei, C., Zhang, H., & Duan, H. (2020). Effect of catalytic-reactive rejuvenator on structure and properties of aged SBS modified asphalt binders. Construction and Building Materials, 246, 118531. https://doi.org/10.1016/j.conbuildmat.2020.118531

[17] Zhu, J., Birgisson, B., & Kringos, N. (2014). Polymer modification of bitumen: Advances and challenges. European Polymer Journal, 54, 18–38. https://doi.org/10.1016/j.eurpolymj.2014.02.005

[18] Kakar, M. R., Hamzah, M. O., Akhtar, M. N., & Woodward, D. (2016). Surface free energy and moisture susceptibility evaluation of asphalt binders modified with surfactant-based chemical additive. Journal of Cleaner Production, 112, 2342–2353. https://doi.org/10.1016/j.jclepro.2015.10.101

[19] Dyuryagina, A., Byzova, Y., Ostrovnoy, K., & Vasiliev, A. (2024). Increasing the adhesion of bitumen to the surface of mineral fillers through modification with a recycled polymer and surfactant obtained from oil refining waste. Polymers, 16(5), 714. https://doi.org/10.3390/polym16050714

[20] Cheraghian, G., & Wistuba, M. P. (2020). The role of additives in warm mix asphalt technology: An insight into their mechanisms. Nanomaterials.